Galleria mellonella as a host model to study *Candida glabrata* virulence and antifungal efficacy

Lauren Ames, Sarah Duxbury, Bogna Pawlowska, Hsueh-lui Ho, Ken Haynes, and Steven Bates*

Biosciences, College of Life and Environmental Sciences, University of Exeter, Exeter EX4 4QD, UK

Keywords: *Galleria mellonella, Candida glabrata*, virulence, host model; fungal pathogenesis

* Correspondence to: Steven Bates; E-mail: s.bates@ex.ac.uk

Candida species are common human fungal pathogens causing a wide range of clinical diseases, ranging from superficial infections to life-threatening systemic disease. Superficial infections include vaginal candidiasis which affects over 75% of women during their lifetime with 5% of women suffering debilitating recurrent infections. [1, 2] Life-threatening systemic *Candida* disease is the fourth most common nosocomial blood stream infection, affecting those undergoing chemotherapy, recovering from surgical procedures or major burns, transplant recipients and AIDs patients. The crude mortality rate associated with these infections is high, ranging from 46-75%, and current estimates suggest at least 400,000 life-threatening infections occur annually. [1, 3-6] *Candida albicans* is the predominant cause of invasive candidiasis, although in the last three decades there has been a rise in the incidence of non-*albicans Candida* species with *Candida glabrata*, *Candida parapsilosis* and *Candida tropicalis* being the other main agents causing disease. Of these, *C. glabrata* is the second most common cause of invasive candidiasis in the USA and Central and Northern Europe, and it has been associated with higher hospital costs. [5, 7-9] The basis of this increasing incidence of *C. glabrata* is not fully understood, however, it could be partially attributed to the higher innate tolerance *C. glabrata* displays to azole antifungals alongside its greater potential to develop drug resistance coincident with therapy. [10, 11]

Murine models of infection are typically viewed as the gold standard for fungal virulence studies. However, although these models allow the host-pathogen interaction to be studied *in vivo* they do come with caveats associated with cost, legislation, and careful ethical considerations. Furthermore, with the development of large scale mutant libraries alternative, more ethically acceptable, models are required to identify interesting virulence targets whilst limiting the use of mice. [12, 13] Given the caveats associated with murine models of infection mini-host models, mainly invertebrates, have been explored as alternative models for fungal infection. These models include amoeba (*Dictyostellium discoideum*), nematodes (*Caenorhabditis elegans*), fruit fly (*Drosophila melanogaster*) and the greater wax moth larvae (*Galleria mellonella*). [14-16] *G. mellonella*, a lepidopteran, was

first described as a mini-host for *Candid*a species by Kavanagh and co-workers [17, 18], and has received particular attention as an alternative host as it displays some important advantages. The *G. mellonella* larvae can be incubated at 37 ºC, allowing virulence to be studied at human body temperature, and an exact inoculum of the pathogen can be delivered by injection. Furthermore, the assays are inexpensive and simple to perform, allowing large numbers of larvae to be infected and thus increasing the statistical power of the assay. Finally some aspects of the *G. mellonella* immune response show similarities with the innate immune response of mammals. [14, 15, 19] Given these advantages the model has now been developed for a wide range of fungal pathogens, including a number of *Candida* species. [17, 18, 20-22]

To study *C. glabrata* infection in mice immunosuppression is usually required, and fungal burdens and persistence are normally employed as a parameter for virulence due to the absence of mortality. [23] This, along with the recent development of large scale mutant libraries, makes alternative models for studying *C. glabrata* virulence an attractive proposition. Initial reports on establishing the *G. mellonella* model for testing the virulence of *Candida* species only reported a low level of killing of larvae by *C. glabrata*. [18, 24, 25] However, we and others [26, 27] have now shown that a faster rate of killing by *C. glabrata* is seen when using a higher pathogen concentration. In this work we provide the first detailed report on the ability of *C. glabrata* to grow and cause lethal infections in *G. mellonella* in a dose dependent manner. Furthermore, we have shown that this model can be used to assess the relative virulence of *C. glabrata* clinical isolates, and that the analysis of mutant strains demonstrates an overlap with results published using murine infection models. Finally, we have shown that antifungal efficacy in the *G. mellonella* model correlates with the *in vitro* susceptibility profile of *C. glabrata*. Therefore, the *G. mellonella* model can be used to study both *C. glabrata* virulence and antifungal efficacy.

In order to evaluate *G. mellonella* as a host model for *C. glabrata* infection we first infected larvae with the commonly used wild type reference strain ATCC2001 [28] at a range of

different inoculum levels (7.5×10^5, 1×10^6, 2.5×10^6, 5×10^6 and 7.5×10^6 cells/larva). For this, groups of twenty healthy larvae (0.25-0.35g) were inoculated with 10 µl of cell suspension through injection into the haemocoel with a Hamilton syringe through the last left pro-leg. Following infection larvae were incubated in the dark at 37 ºC and survival, based on response to physical stimulation, was monitored daily for seven days. Larvae inoculated with PBS were used as uninfected controls and resulted in no deaths (data not shown), and all assays were performed at least three times independently. The results from this clearly demonstrated that *C. glabrata* can kill the larvae in a dose dependent fashion (Fig. 1A). For example, infection with 2.5×10^6 cells/larva gave a mean survival time of 3.45 ± 0.28 days compared to 1.63 ± 0.13 days with an infective dose of 7.5×10^6 cells/larva ($P<0.0001$). The infective dose required for *C. glabrata* to kill *G. mellonella* larvae was however approximately ten fold higher than the dose of *C. albicans* required to cause death, where an infective dose of 2×10^5 cells/larva *C. albicans* NGY152 [29] cells resulted in a mean survival time of 2.95 ± 0.21 days (data not shown) similar to previous reports. [17, 18, 22] Similar findings have been seen with other *Candida* species, [20-22] and for *C. glabrata* is perhaps in keeping with its differing virulence properties favouring stealth and evasion over aggressive invasion. [23, 30] Given the high dose of *C. glabrata* required to cause *G. mellonella* killing we also evaluated the survival of larvae inoculated with heat-killed yeast cells (incubated at 75 ºC for 20 min before use), to ensure that killing was not due to other factors such as toxic shock. No larval death was seen following infection with heat-killed cells at 5×10^6 cells/larva (data not shown); therefore the killing of larvae in this model is dependent on viable *C. glabrata* cells.

Temperature has been seen to impact on the outcome of *G. mellonella* infection for some fungal species, with both *C. albicans* and *C. tropicalis* displaying faster killing following incubation at 37 ºC rather than 30 ºC whereas killing rates following *C. krusei* infection were not affected by temperature. [21, 22, 31] To determine if temperature also impacts on the virulence of *C. glabrata* we compared the virulence of *C. glabrata* ATCC2001 at 30 and 37 ºC. At the intermediate infective doses of both 1×10^6 and 2.5×10^6 cells/larva *C. glabrata*

virulence was significantly decreased at 30 ºC compared to 37 ºC (Fig. 1B, P<0.005). For example, with the 2.5 x 10^6 cells/larva dose the mean survival time at 30 ºC was 4.65 ± 0.33 days compared to 3.45 ± 0.28 days at 37 ºC. However, no significant impact of temperature was seen when higher infective doses were employed, suggesting this limitation can be overcome. The increased mortality seen at higher temperatures with intermediate infective doses may be the result of the impact of temperature on both the growth and virulence properties of the pathogen, plus the effect of temperature on the immune response of the larvae. [32]

Following infection with *C. glabrata* larvae quickly developed a brown-black colouration, indicative of the accumulation of melanin as part of the insect innate immune response. To quantify this hemolymph was collected from infected larvae, at 2 and 6 hours post infection, following established methods. [33] The extent of melanisation was then determined through measuring the hemolymph optical density at 405 nm, which correlates with its visual appearance and has been used previously to quantify laccase activity. [22] Through this the extent of melanisation was seen to be dependent on both the infective dose of *C. glabrata* and time post infection (Fig 1C). In addition to the activation of melanisation, previous work has demonstrated that the density of free hemocytes in the hemolymph is decreased following infection with *C. albicans* and other microbes. [21, 22, 24] This decrease was seen to correlate with susceptibility to infection, and is thought to be the result of nodulation or clumping of hemocytes, pathogens and melanised debris at the infection site. [19] Following infection with *C. glabrata*, at 2.5 x 10^6 cells/larva, we also saw a significant decrease in total hemocyte cell density, with levels falling from 8.5 x 10^6 ± 2.0 x 10^6 cells/ml for PBS inoculated control larvae to 4.6 x 10^6 ± 1.2 x 10^6 (54%; p<0.01) and 2.7 x 10^6 ± 9.7 x 10^5 (33%; p<0.005) at 2 and 6 hours post infection respectively. Overall therefore, with the activation of melanisation and the drop in free hemocyte density, it is clear that the larvae mount a defence response following *C. glabrata* infection.

To follow the progress of infection we also determined the fungal burdens in *G. mellonella*, at 0, 6, 24, 48 and 72 h post infection, following inoculation with $2.5x10^6$ cells/larva *C. glabrata* ATCC2001. For this nine larvae were taken at each time point, briefly washed in 70 % ethanol followed by sterile water, and then placed into 15 ml screw-cap tubes with four 3 mm stainless steel balls and 1 ml PBS. The tissue was then homogenised through three rounds of shaking for 20 s at 4 m/s in a Fastprep-24 (MP Biomedicals). The resulting homogenate was then suspended in 14 ml PBS and serial dilutions prepared and inoculated onto YEPD-chloramphenicol (100 µg/ml) plates. Immediately following infection the detectable fungal burden was $5.8\ x10^5 \pm 3.4\ x\ 10^5$ CFU/larvae, and initially remained fairly constant only reaching $8.5\ x10^5 \pm 6\ x10^5$ CFU/larvae at 6 h post infection. However, by 24 h, when larvae began to succumb to infection, fungal burdens had risen ~20 fold to $1.2\ x10^7 \pm 9.4\ x10^6$ CFU/larvae and continued to rise at 48 and 72 h post infection (Fig. 1D), demonstrating growth of the *C. glabrata* in the host.

In addition to testing the ability of *C. glabrata* ATCC2001 to cause lethal infection in *G. mellonella* we also screened a further five clinical isolates (BG2, Cg1184, Cg85/038, Cg11088A and NCPF3605) [34-37], including the other commonly used isolate BG2, at three infective doses ($1.25\ x\ 10^6$, $2.5\ x\ 10^6$ and $5\ x\ 10^6$ cells/larva; Fig. 2). All strains demonstrated a dose dependent response, and four of these strains (BG2, Cg1184, Cg85/038 and Cg11088A) demonstrated a very similar level of virulence to ATCC2001. Indeed when comparing the different infective doses the only significant difference was the slight increase in virulence seen with strain Cg1184 at the $5\ x\ 10^6$ cells/larva dose compared to BG2 ($P<0.005$) and Cg11088A ($P<0.05$). Therefore the majority of *C. glabrata* isolates tested show broadly similar levels of virulence in this model. The only key exception was the NCPF3605 strain which, at all infective doses tested, was clearly highly attenuated in virulence compared to all the other isolates ($P<0.0001$) only causing 22.5% ± 9.6% killing of larvae by 7 days at the highest dose tested. A recent comparison of the growth of this strain and ATCC2001, at varying glucose concentrations, demonstrated distinct differences, with

NCPF3605 displaying a faster growth rate but at the cost of entering stationary phase at a lower cell density. [38] General fitness defects may therefore impact on the virulence of *C. glabrata* in this model and, importantly, the *G. mellonella* model can be used to detect differences in the virulence potential of *C. glabrata* strains.

Auxotrophic markers are commonly used for selection during the genetic modification of *Candida* species. However, *in C. albicans* it is well recognised that *ura3* auxotrophy causes virulence to be highly attenuated in the mouse model of infection, and that the level of expression of *URA3* can also impact on virulence. [29, 39] In this work we have demonstrated that *ura3* auxotrophy has a similar impact on the virulence of *C. glabrata* in the *G. mellonella* infection model. *G. mellonella* infected with 2. 5 x10^6 cells/larva of wild type *C. glabrata* (ATCC2001) demonstrated a mean survival time of 2.90 ± 0.19 days compared to 6.39 ± 0.13 days ($p<0.0001$) for those infected with a *ura3* auxotroph (strain 2001U [40]). Given the known issues with *ura3* auxotrophy in *C. albicans*, most work in *C. glabrata* uses other auxotrophic markers that have been shown not to impact on virulence in mice. [23, 41] We therefore also screened *his3*, *leu2* and *trp1* single mutants (strains 2001H, 2001L and 2001T respectively) and a *his3*, *leu2*, *trp1* triple mutant (strain 2001HTL). [41] Similar to the situation in a mouse model, loss of *HIS3* or *LEU2* did not impact on microbial virulence within the *G. mellonella* model (data not shown). However, in our model we did detect a subtle, but significant, attenuation of virulence in the *trp1* single (mean survival time 3.67 ± 0.20 days, $p=0.0173$) and *his3*, *leu2*, *trp1* triple null mutant (mean survival time 3.87 ± 0.20 days, $p=0.0020$) compared to the wild type strain ATCC2001 (mean survival time of 2.90 ± 0.19 days). It is tempting to attribute the lower virulence of the triple mutant to its loss of *trp1*; however, as we did not test this empirically we cannot rule out the possibility that the combined auxotrophies also impact on fitness and ultimately virulence. Overall, we would therefore suggest that when using this model it is important to ensure appropriate control strains, displaying the same auxotrophies, are employed.

In order to assess the utility of this model to screen defined mutants for virulence defects we also carried out virulence assays with fourteen deletion mutants, including eight whose phenotype in a mouse model of infection has previously been reported. These included twelve mutants associated with *C. glabrata* stress responses (Δ*ste50*, Δ*ste20*, Δ*hog1*, Δ*skn7*, Δ*yap1*, Δ*cta1*, Δ*rim101*, Δ*yps1*, Δ*msn2*, Δ*msn4*, Δ*cst6* and Δ*slt2*) [41-43] plus two glycosylation mutants (Δ*mnn2* and Δ*anp1*) [44] that have previously been shown to be hypervirulent in mice. In order to increase the statistical power of the assay we used fifty larvae per replicate, and selected one infective dose (2.5 x 10^6 cells/larva) which would allow either an increase or decrease in virulence potential to be observed. Virulence was then compared to the relevant wild type strain (2001HTL, 2001H or HT6 [41, 43]), selected based on the genetic background of the mutant. Through this analysis we identified five mutants that demonstrated a mild but significant attenuation in virulence, including Δ*ste50*, Δ*ste20*, Δ*hog1* in the Hog pathway, Δ*slt2* in the cell wall integrity pathway and Δ*skn7* involved in oxidative stress resistance (Table 1). The level of attenuation in these mutants was generally subtle, but shown to be significant through the benefit of being able to infect a large number of larvae in order to increase the statistical power of the assay. Of these mutants four, Δ*ste20*, Δ*hog1*, Δ*slt2* and Δ*skn7,* have previously been tested in a mouse model of systemic infection where they also displayed a mild (Δ*ste20*, Δ*slt2* and Δ*skn7*) to moderate (Δ*hog1*) attenuation of virulence. [45-48] For *STE50* this is the first report of its importance in virulence, and the phenotype displayed by the Δ*ste50* mutant is in keeping with the overall importance of the Hog1 pathway. Furthermore, the large scale analysis of *C. glabrata* mutants in the *Drosophila* infection model [13] also identified both the Hog1 and cell wall integrity pathways as playing a key role in virulence, therefore the importance of these pathways has been consistently demonstrated in three different infection models. The remaining mutants (Δ*yap1*, Δ*cta1*, Δ*rim101*, Δ*yps1*, Δ*msn2*, Δ*msn4* and Δ*cst6*; Table 1) displayed no significant defect in virulence, and of these two (Δ*yap1* and Δ*cta1*) have also previously been reported to display no virulence defect in mice. [49, 50] In addition to the stress response mutants we also

screened two glycosylation mutants (Δ*mnn2* and Δ*anp1*) [44] that have previously been shown to demonstrate increased virulence in a mouse model of infection. Intriguingly, these deletion mutants also displayed increased virulence in the *G. mellonella* model whilst their complemented strains demonstrated wild type virulence (Table 1). The molecular basis of this hypervirulence is currently not clear, but the mutants are known to be hyperadherent and potentially elicit a septic-shock like response. [44] This may therefore suggest that either similar components are involved in the recognition of the pathogen by *G. mellonella* or common adhesins play a role in both models. Overall, of the fourteen mutants tested in this study eight have previously been screened in mice and we have shown all to display comparable phenotypes in the *G. mellonella* model, plus confirm the importance of the Hog1 and cell wall integrity pathways in virulence. This correlation is very encouraging and suggests that this model has the potential to be used to screen for novel virulence factors in *C. glabrata*

In order to facilitate the future use of this model for comparing mutant strains, potentially through large scale screening efforts, we also calculated a larval virulence index (LVI) as a measure of virulence for the set of fourteen mutants tested. For this we followed the methodology established for use with the *Drosophila* infection model. [13, 41] Survival curves were initially fitted to a Weibull distribution, then the time of 50% larval survival (LT_{50}) determined and from this the LVI presented as the $\log_2$ ratio of mutant and corresponding wild type control (Table 1). The LT_{50} values determined for the different strains were, as expected, in very strong agreement with their mean survival times (Spearman's rho=0.99, P<0.00001). Furthermore, applying the cut-offs established by Brunke *et al*. [13] for increased or decreased virulence (virulence index ±0.5), six of the seven mutants we identified as displaying altered virulence through the traditional log rank tests were also highlighted by this approach. The mutant not highlighted, Δ*ste20*, was on the verge of detection with a LVI of -0.46 and was also the least attenuated in virulence through the traditional log rank test. Overall, therefore, this modelling approach gives a strong quantitative measure of virulence,

and may facilitate the future use of this model in the large scale screening of available *C. glabrata* deletion libraries. [41]

Finally, we also tested the efficacy of fluconazole, amphotericin B, and caspofungin against *C. glabrata* in the *G. mellonella* model and compared this to *C. albicans*. *C. glabrata* is well recognised for displaying a higher innate tolerance to azole antifungals than *C. albicans.* [10, 11] Consistent with this, although *C. albicans* NGY152 was highly sensitive to fluconazole *in vitro* the *C. glabrata* strain ATCC2001 displayed a high MIC of 32 µg/ml, whereas for caspofungin and amphotericin B both were acutely sensitive. We next tested the efficacy of these antifungals in the *G. mellonella* model at clinically relevant doses that did not cause toxicity in the model (data not shown). For this, larvae were infected with 1 x 10^5 cells/larva *C. albicans* NGY152 or 1.25 x 10^6 cells/larva *C. glabrata* ATCC2001 and antifungals administered 30 min post infection through a second 10 µl injection into the pro-leg adjacent to the site of initial infection. Untreated controls received a second injection of PBS. For *G. mellonella* infected with *C. albicans,* treatment with fluconazole at all concentrations tested (3, 6, and 12 mg/kg) promoted survival (Fig 3A; $P<0.0001$). In contrast treatment with the same levels of fluconazole provided no protection against *C. glabrata* infection (Fig. 3B). Amphotericin B at both 2 and 4 mg/kg also protected larvae against infection by *C. albicans* (Fig. 3C; $P<0.0001$), whereas only the highest concentration (4 mg/kg) provided significant protection against *C. glabrata* (Fig. 3D; $P<0.0001$). Finally, caspofungin also protected *G. mellonella* against *C. albicans* infection at all concentrations tested (Fig. 3E, 1 mg/kg $P<0.005$; 2 and 4 mg/kg $P<0.0001$), whereas again only the higher doses of 2 and 4 mg/kg provided significant protection against *C. glabrata* infection (Fig. 3F, $P<0.0001$). We therefore saw a clear correlation between *in vitro* susceptibility and *in vivo* efficacy in this model for *C. glabrata*, consistent with previous studies demonstrating the potential of the *G. mellonella* model to be used in testing the toxicity and efficacy of antifungal agents for a range of fungal pathogens. [21, 22, 31, 51, 52] Interestingly, although amphotericin B and caspofungin did provide protection against *C. glabrata,* in both cases a higher dose of

antifungal was required to achieve efficacy than for treatment of *C. albicans*. A similar profile was seen following infection with *C. krusei* and this was associated with the strain tested, although being susceptible, demonstrating reduced susceptibility compared to the *C. albicans* control strain. [22] In this work however, the *C. glabrata* and *C. albicans* strains employed demonstrated very similar susceptibility profiles towards amphotericin B and caspofungin. The basis of this subtle but consistent *in vivo* susceptibility shift is therefore not clear. It could simply be due to the requirement of a tenfold higher infective dose for *C. glabrata* compared to *C. albicans*, which may result in the need for a higher drug concentration, or alternatively it could be suggestive of *C. glabrata* displaying a higher *in vivo* tolerance towards antifungals.

Infection models utilising *G. mellonella* are generally gaining acceptance and have now been established for a range of fungal pathogens. As previously discussed these models present some advantages through being more ethically acceptable, inexpensive allowing the use of more test subjects to increase the statistical power of the assay, alongside the easy manipulation of larvae and ability to assay at 37 ºC. There are however some disadvantages such as no complete genome sequence and the lack of genetic tractability in *G. mellonella*, plus an inherent level of variability in the quality of larvae from suppliers. Finally, as with any infection model, it is unlikely that all virulence attributes involved in mammalian infection will demonstrate similar importance in the *G. mellonella* system. Overall however we would conclude that *G. mellonella* is an attractive and simple model for following *C. glabrata* infection. High doses are initially required to cause an infection, but once established a simple to follow lethal infection coupled with growth of the pathogen and a detectable host response is seen. Furthermore, through the mutants tested, we saw a good level of correlation with murine models suggesting that this system has the potential to be used to screen for novel virulence factors in this important pathogen. Finally, as has been seen with other fungal pathogens, this system can clearly be employed for the *in vivo* evaluation of antifungal agents.

Acknowledgments

We thank Sukrit Silas (Stanford University) for providing information on the application of the modelling approach. This work was supported in part by the Wellcome Trust Strategic Award for Medical Mycology and Fungal Immunology 097377/Z/11/Z.

References

1. Brown GD, Denning DW, Gow NA, Levitz SM, Netea MG, White TC. Hidden killers: human fungal infections. Sci Transl Med 2012; 4:165rv13.

2. Sobel JD. Vulvovaginal candidosis. Lancet 2007; 369:1961-71.

3. Leroy O, Gangneux JP, Montravers P, Mira JP, Gouin F, Sollet JP, Carlet J, Reynes J, Rosenheim M, Regnier B, et al. Epidemiology, management, and risk factors for death of invasive *Candida* infections in critical care: a multicenter, prospective, observational study in France (2005-2006). Crit Care Med 2009; 37:1612-8.

4. Perlroth J, Choi B, Spellberg B. Nosocomial fungal infections: epidemiology, diagnosis, and treatment. Med Mycol 2007; 45:321-46.

5. Pfaller M, Neofytos D, Diekema D, Azie N, Meier-Kriesche HU, Quan SP, Horn D. Epidemiology and outcomes of candidemia in 3648 patients: data from the Prospective Antifungal Therapy (PATH Alliance(R)) registry, 2004-2008. Diagn Microbiol Infect Dis 2012; 74:323-31.

6. Pfaller MA, Diekema DJ. Epidemiology of invasive mycoses in North America. Crit Rev Microbiol 2010; 36:1-53.

7. Diekema D, Arbefeville S, Boyken L, Kroeger J, Pfaller M. The changing epidemiology of healthcare-associated candidemia over three decades. Diagn Microbiol Infect Dis 2012; 73:45-8.

8. Moran C, Grussemeyer CA, Spalding JR, Benjamin DK, Jr., Reed SD. Comparison of costs, length of stay, and mortality associated with *Candida glabrata* and *Candida albicans* bloodstream infections. Am J Infect Control 2010; 38:78-80.

9. Quindos G. Epidemiology of candidaemia and invasive candidiasis. A changing face. Rev Iberoam Micol 2014; 31:42-8.

10. Pfaller MA, Diekema DJ. Epidemiology of invasive candidiasis: a persistent public health problem. Clin Microbiol Rev 2007; 20:133-63.

11. Pfaller MA, Diekema DJ, Gibbs DL, Newell VA, Barton R, Bijie H, Bille J, Chang SC, da Luz Martins M, Duse A, et al. Geographic variation in the frequency of isolation and fluconazole and voriconazole susceptibilities of *Candida glabrata*: an assessment from the ARTEMIS DISK Global Antifungal Surveillance Program. Diagn Microbiol Infect Dis 2010; 67:162-71.

12. Amorim-Vaz S, Delarze E, Ischer F, Sanglard D, Coste AT. Examining the virulence of *Candida albicans* transcription factor mutants using *Galleria mellonella* and mouse infection models. Front Microbiol 2015; 6:367.

13. Brunke S, Quintin J, Kasper L, Jacobsen ID, Richter ME, Hiller E, Schwarzmuller T, d'Enfert C, Kuchler K, Rupp S, et al. Of mice, flies--and men? Comparing fungal infection models for large-scale screening efforts. Dis Model Mech 2015; 8:473-86.

14. Chamilos G, Lionakis MS, Lewis RE, Kontoyiannis DP. Role of mini-host models in the study of medically important fungi. Lancet Infect Dis 2007; 7:42-55.

15. Desalermos A, Fuchs BB, Mylonakis E. Selecting an invertebrate model host for the study of fungal pathogenesis. PLoS Pathog 2012; 8:e1002451.

16. Maccallum DM. Hosting infection: experimental models to assay *Candida* virulence. Int J Microbiol 2012; 2012:363764.

17. Brennan M, Thomas DY, Whiteway M, Kavanagh K. Correlation between virulence of *Candida albicans* mutants in mice and *Galleria mellonella* larvae. FEMS Immunol Med Microbiol 2002; 34:153-7.

18. Cotter G, Doyle S, Kavanagh K. Development of an insect model for the *in vivo* pathogenicity testing of yeasts. FEMS Immunol Med Microbiol 2000; 27:163-9.

19. Browne N, Heelan M, Kavanagh K. An analysis of the structural and functional similarities of insect hemocytes and mammalian phagocytes. Virulence 2013; 4:597-603.

20. Gago S, Garcia-Rodas R, Cuesta I, Mellado E, Alastruey-Izquierdo A. *Candida parapsilosis*, *Candida orthopsilosis*, and *Candida metapsilosis* virulence in the non-conventional host *Galleria mellonella*. Virulence 2014; 5:278-85.

21. Mesa-Arango AC, Forastiero A, Bernal-Martinez L, Cuenca-Estrella M, Mellado E, Zaragoza O. The non-mammalian host *Galleria mellonella* can be used to study the virulence of the fungal pathogen *Candida tropicalis* and the efficacy of antifungal drugs during infection by this pathogenic yeast. Med Mycol 2013; 51:461-72.

22. Scorzoni L, de Lucas MP, Mesa-Arango AC, Fusco-Almeida AM, Lozano E, Cuenca-Estrella M, Mendes-Giannini MJ, Zaragoza O. Antifungal efficacy during *Candida krusei* infection in non-conventional models correlates with the yeast *in vitro* susceptibility profile. PLoS One 2013; 8:e60047.

23. Jacobsen ID, Brunke S, Seider K, Schwarzmuller T, Firon A, d'Enfert C, Kuchler K, Hube B. *Candida glabrata* persistence in mice does not depend on host immunosuppression and is unaffected by fungal amino acid auxotrophy. Infect Immun 2010; 78:1066-77.

24. Bergin D, Brennan M, Kavanagh K. Fluctuations in haemocyte density and microbial load may be used as indicators of fungal pathogenicity in larvae of *Galleria mellonella*. Microbes Infect 2003; 5:1389-95.

25. Junqueira JC, Fuchs BB, Muhammed M, Coleman JJ, Suleiman JM, Vilela SF, Costa AC, Rasteiro VM, Jorge AO, Mylonakis E. Oral *Candida albicans* isolates from HIV-positive individuals have similar *in vitro* biofilm-forming ability and pathogenicity as invasive *Candida* isolates. BMC Microbiol 2011; 11:247.

26. Borghi E, Andreoni S, Cirasola D, Ricucci V, Sciota R, Morace G. Antifungal resistance does not necessarily affect *Candida glabrata* fitness. J Chemother 2014; 26:32-6.

27. Santos R, Costa C, Mil-Homens D, Romao D, de Carvalho CC, Pais P, Mira NP, Fialho AM, Teixeira MC. The multidrug resistance transporters *Cg*Tpo1_1 and *Cg*Tpo1_2 play a role in virulence and biofilm formation in the human pathogen *Candida glabrata*. Cell Microbiol 2016; 19:e12686.

28. Dujon B, Sherman D, Fischer G, Durrens P, Casaregola S, Lafontaine I, De Montigny J, Marck C, Neuveglise C, Talla E, et al. Genome evolution in yeasts. Nature 2004; 430:35-44.

29. Brand A, MacCallum DM, Brown AJ, Gow NA, Odds FC. Ectopic expression of *URA3* can influence the virulence phenotypes and proteome of *Candida albicans* but can be overcome by targeted reintegration of *URA3* at the *RPS10* locus. Eukaryot Cell 2004; 3:900-9.

30. Brunke S, Hube B. Two unlike cousins: *Candida albicans* and *C. glabrata* infection strategies. Cell Microbiol 2013; 15:701-8.

31. Mylonakis E, Moreno R, El Khoury JB, Idnurm A, Heitman J, Calderwood SB, Ausubel FM, Diener A. *Galleria mellonella* as a model system to study *Cryptococcus neoformans* pathogenesis. Infect Immun 2005; 73:3842-50.

32. Kavanagh K, Reeves EP. Exploiting the potential of insects for *in vivo* pathogenicity testing of microbial pathogens. FEMS Microbiol Rev 2004; 28:101-12.

33. Fuchs BB, O'Brien E, Khoury JB, Mylonakis E. Methods for using *Galleria mellonella* as a model host to study fungal pathogenesis. Virulence 2010; 1:475-82.

34. Cormack BP, Falkow S. Efficient homologous and illegitimate recombination in the opportunistic yeast pathogen *Candida glabrata*. Genetics 1999; 151:979-87.

35. Haynes KA, Westerneng TJ. Rapid identification of *Candida albicans*, *C. glabrata*, *C. parapsilosis* and *C. krusei* by species-specific PCR of large subunit ribosomal DNA. J Med Microbiol 1996; 44:390-6.

36. Haynes KA, Westerneng TJ, Fell JW, Moens W. Rapid detection and identification of pathogenic fungi by polymerase chain reaction amplification of large subunit ribosomal DNA. J Med Vet Mycol 1995; 33:319-25.

37. Zhou PB, Thiele DJ. Isolation of a metal-activated transcription factor gene from *Candida glabrata* by complementation in *Saccharomyces cerevisiae*. Proc Natl Acad Sci U S A 1991; 88:6112-6.

38. Reding-Roman C, Hewlett M, Duxbury S, Gori F, Gudelj I, Beardmore R. The unconstrained evolution of fast and efficient antibiotic-resistant bacterial genomes. Nat Ecol Evol 2017; 1:0050.

39. Staab JF, Sundstrom P. *URA3* as a selectable marker for disruption and virulence assessment of *Candida albicans* genes. Trends Microbiol 2003; 11:69-73.

406 40. Kitada K, Yamaguchi E, Arisawa M. Cloning of the *Candida glabrata TRP1*
407 and *HIS3* genes, and construction of their disruptant strains by sequential integrative
408 transformation. Gene 1995; 165:203-6.
409 41. Schwarzmuller T, Ma B, Hiller E, Istel F, Tscherner M, Brunke S, Ames L,
410 Firon A, Green B, Cabral V, et al. Systematic phenotyping of a large-scale *Candida*
411 *glabrata* deletion collection reveals novel antifungal tolerance genes. PLoS Pathog
412 2014; 10:e1004211.
413 42. Roetzer A, Klopf E, Gratz N, Marcet-Houben M, Hiller E, Rupp S, Gabaldon T,
414 Kovarik P, Schuller C. Regulation of *Candida glabrata* oxidative stress resistance is
415 adapted to host environment. FEBS Lett 2011; 585:319-27.
416 43. Weig M, Haynes K, Rogers TR, Kurzai O, Frosch M, Muhlschlegel FA. A
417 *GAS*-like gene family in the pathogenic fungus *Candida glabrata*. Microbiology 2001;
418 147:2007-19.
419 44. West L, Lowman DW, Mora-Montes HM, Grubb S, Murdoch C, Thornhill MH,
420 Gow NA, Williams D, Haynes K. Differential virulence of *Candida glabrata*
421 glycosylation mutants. J Biol Chem 2013; 288:22006-18.
422 45. Calcagno AM, Bignell E, Rogers TR, Canedo M, Muhlschlegel FA, Haynes K.
423 *Candida glabrata* Ste20 is involved in maintaining cell wall integrity and adaptation to
424 hypertonic stress, and is required for wild-type levels of virulence. Yeast 2004;
425 21:557-68.
426 46. Miyazaki T, Inamine T, Yamauchi S, Nagayoshi Y, Saijo T, Izumikawa K, Seki
427 M, Kakeya H, Yamamoto Y, Yanagihara K, et al. Role of the Slt2 mitogen-activated
428 protein kinase pathway in cell wall integrity and virulence in *Candida glabrata*. FEMS
429 Yeast Res 2010; 10:343-52.

47. Saijo T, Miyazaki T, Izumikawa K, Mihara T, Takazono T, Kosai K, Imamura Y, Seki M, Kakeya H, Yamamoto Y, et al. Skn7p is involved in oxidative stress response and virulence of *Candida glabrata*. Mycopathologia 2010; 169:81-90.

48. Srivastava VK, Suneetha KJ, Kaur R. The mitogen-activated protein kinase *Cg*Hog1 is required for iron homeostasis, adherence and virulence in *Candida glabrata*. FEBS J 2015; 282:2142-66.

49. Chen KH, Miyazaki T, Tsai HF, Bennett JE. The bZip transcription factor *Cg*ap1p is involved in multidrug resistance and required for activation of multidrug transporter gene *CgFLR1* in *Candida glabrata*. Gene 2007; 386:63-72.

50. Cuellar-Cruz M, Briones-Martin-del-Campo M, Canas-Villamar I, Montalvo-Arredondo J, Riego-Ruiz L, Castano I, De Las Penas A. High resistance to oxidative stress in the fungal pathogen *Candida glabrata* is mediated by a single catalase, Cta1p, and is controlled by the transcription factors Yap1p, Skn7p, Msn2p, and Msn4p. Eukaryot Cell 2008; 7:814-25.

51. Kelly J, Kavanagh K. Caspofungin primes the immune response of the larvae of *Galleria mellonella* and induces a non-specific antimicrobial response. J Med Microbiol 2011; 60:189-96.

52. Li DD, Deng L, Hu GH, Zhao LX, Hu DD, Jiang YY, Wang Y. Using *Galleria mellonella*-*Candida albicans* infection model to evaluate antifungal agents. Biol Pharm Bull 2013; 36:1482-7.

451 **Table 1. Virulence of *C. glabrata* mutants in the *G. mellonella* model.**

Strain	Mean Survival Time (days)	Log rank test (P value)	LT_{50} (days)	L.V.I.
Wild type (2001HTL) [41]	2.41 ± 0.12	-	1.37	-
Δ*hog1* [41]	3.30 ± 0.41	<0.005	2.31	-0.52
Δ*skn7* [41]	3.87 ± 0.25	<0.0001	3.30	-0.88
Δ*rim101* [41]	2.27 ± 0.09	N.S.	1.34	0.02
Δ*yps1* [41]	2.87 ± 0.11	N.S.	1.84	-0.30
Wild type (2001HTL) [41]	2.32 ± 0.12	-	1.29	-
Δ*ste50* [41]	3.99 ± 0.10	<0.0001	3.22	-0.92
Δ*slt2* [41]	3.26 ± 0.23	<0.0005	2.26	-0.56
Δ*ste20* [41]	3.09 ± 0.19	<0.01	2.04	-0.46
Δ*cta1* [41]	2.41 ± 0.16	N.S.	1.45	-0.12
Wild type (HT6) [43]	2.44 ± 0.19	-	1.42	-
Δ*yap1* [42]	2.57 ± 0.42	N.S.	1.48	-0.04
Wild type (2001H) [41]	3.32 ± 0.37	-	2.30	-
Δ*msn4* [41]	3.40 ± 0.25	N.S.	2.41	-0.05
Δ*cst6* [41]	3.01 ± 0.15	N.S.	2.06	0.11
Δ*msn2* [41]	2.93 ± 0.20	N.S.	1.92	0.18
Wild type (HT6) [43]	3.17 ± 0.28	-	2.20	-
Δ*mnn2* [44]	2.11 ± 0.16	<0.0001	1.22	0.59
Δ*mnn2+MNN2* [44]	3.29 ± 0.48	N.S.	2.30	-0.05
Wild type (HT6) [43]	2.79 ± 0.09	-	1.71	-
Δ*anp1* [44]	1.54 ± 0.16	<0.0001	0.73	0.85
Δ*anp1+ANP1* [44]	2.64 ± 0.13	N.S.	1.57	0.09

452 (L.V.I. Larval virulence index, N.S. Not significant)

453

Figure 1. Virulence of *C. glabrata* in *G. mellonella*. (**A and B**) Survival curves of *G. mellonella* infected with *C. glabrata* ATCC2001 at 7.5 x 10^5 (squares), 1 x 10^6 (triangles), 2.5 x 10^6 (upside-down triangles), 5 x10^6 (diamonds) and 7.5 x 10^6 (circles) cells/larva at 37 ºC (A) and 30 ºC (B). At 37 ºC (A) all infective doses displayed significant differences ($p<0.05$), whereas at 30 ºC (B) all doses displayed significant differences ($p<0.05$) except between the two lowest infective doses (7.5 x 10^5 and 1 x 10^6 cells/larva). (**C**) Larvae were infected with *C. glabrata* ATCC2001 at 1 x 10^6, 2.5 x 10^6, and 5 x10^6 cells/larva and at 2 and 6 hours post infection hemolymph was collected from larvae and OD_{405} determined to quantify melanin production. Larvae inoculated with PBS were used as a control, and asterisks denote a statistically significant difference to the PBS control ($p<0.05$). (**D**) *G. mellonella* were infected with *C. glabrata* ATCC2001 at 2.5 x 10^6 cells/larva and fungal burdens determined at the time points indicated. Scatterplots depict combined results from three independent replicates using nine larvae for each time point.

Figure 2. Virulence of *C. glabrata* clinical isolates in *G. mellonella*. Survival curves of *G. mellonella* infected with *C. glabrata* ATCC2001 (open squares), NCPF3605 (closed squares), BG2 (triangles), Cg1184 (upside-down triangles), Cg85/038 (diamonds), and Cg11088A (circles) at 1 x 10^6 (**A**), 2.5 x 10^6 (**B**), and 5 x10^6 (**C**) cells/larva. At all doses strain NCPF3605 was highly attenuated compared to all other strains ($p<0.0001$); plus at the highest dose (C) a slight but significant increase in virulence was seen for Cg1184 compared to BG2 ($p<0.005$) and Cg11088A ($p<0.05$),

Figure 3. Antifungal efficacy against *C. albicans* and *C. glabrata* in the *G. mellonella* model. Survival curves of *G. mellonella* infected with 1 x 10^5 cells/larva *C. albicans* NGY152 (**A, C and E**) or 1.25 x 10^6 cells/larva *C. glabrata* ATCC2001 (**B, D and F**). (**A and B**) Fluconazole treatment at 0 (squares), 3 (triangle), 6 (diamonds) or 12 mg/kg (circles). (**C, D, E and F**) Amphotericin B or Caspofungin treatment at 0 (squares), 1 (triangle), 2 (diamonds) or 4 mg/kg (circles).

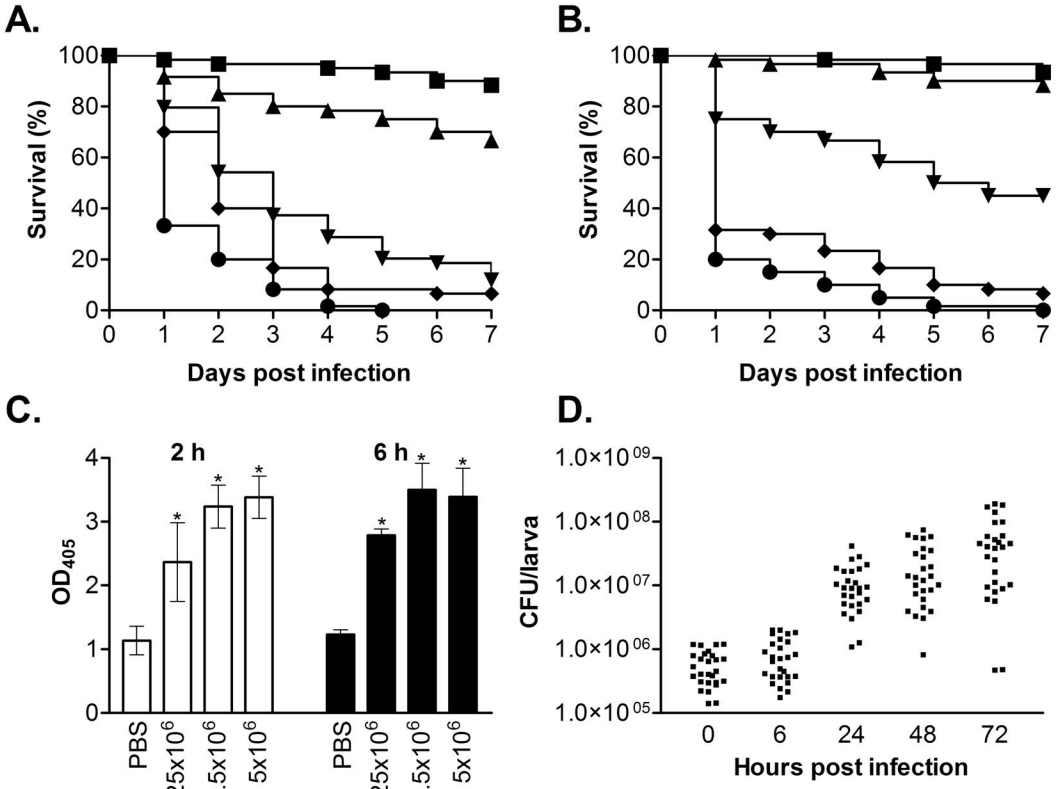
A.
Survival (%)
Days post infection
B.
Survival (%)
Days post infection
C.
2 h
6 h
OD405
PBS
1.25x10^6
2.5x10^6
5x10^6
PBS
1.25x10^6
2.5x10^6
5x10^6
D.
CFU/larva
1.0×10^09
1.0×10^08
1.0×10^07
1.0×10^06
1.0×10^05
Hours post infection

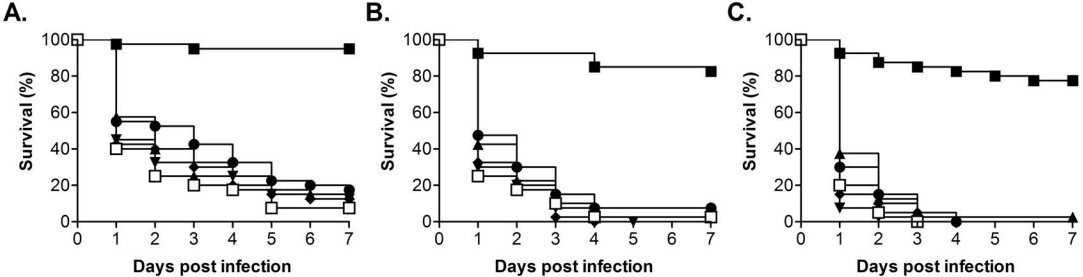
A.
B.
C.
Survival (%)
Days post infection
0
20
40
60
80
100
0 1 2 3 4 5 6 7

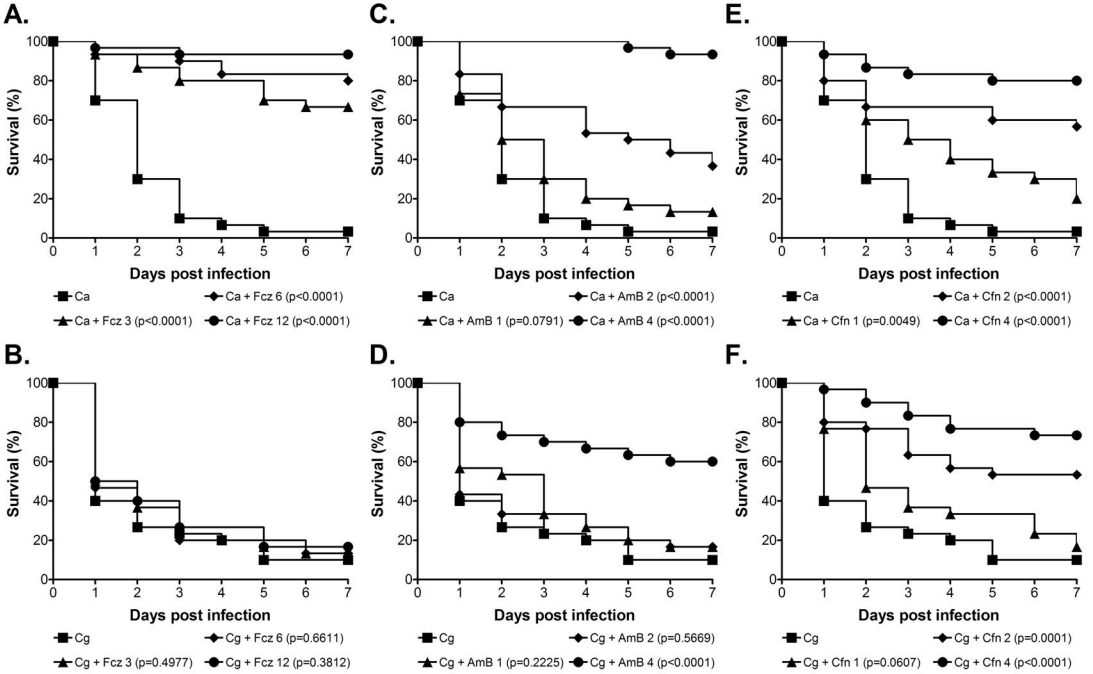
A.
B.
C.
D.
E.
F.
Survival (%)
Days post infection
Ca
Ca + Fcz 6 (p<0.0001)
Ca + Fcz 3 (p<0.0001)
Ca + Fcz 12 (p<0.0001)
Cg
Cg + Fcz 6 (p=0.6611)
Cg + Fcz 3 (p=0.4977)
Cg + Fcz 12 (p=0.3812)
Ca + AmB 2 (p<0.0001)
Ca + AmB 1 (p=0.0791)
Ca + AmB 4 (p<0.0001)
Cg + AmB 2 (p=0.5669)
Cg + AmB 1 (p=0.2225)
Cg + AmB 4 (p<0.0001)
Ca + Cfn 2 (p<0.0001)
Ca + Cfn 1 (p=0.0049)
Ca + Cfn 4 (p<0.0001)
Cg + Cfn 2 (p=0.0001)
Cg + Cfn 1 (p=0.0607)
Cg + Cfn 4 (p<0.0001)